PREDICTION OF BURSTING PRESSURE OF THIN WALLED 316 STAINLESS STEEL TUBES BASED ON ASME B31G CRITERION

A. Chennakesava Reddy

Professor, Department of Mechanical Engineering, JNT University, Hyderabad-500 085, India
dr_acreddy@yahoo.com

Abstract

The objective of the present work was to find the bursting pressure, longitudinal stress and hoop stress of 316F, 316L and 316N stainless steels using ASME B31G criterion. The significance of crack dimensions was optimized using Taguchi techniques. The highly influencing crack dimension was crack depth. The bursting pressure decreased with the increase of crack depth. The bursting pressure was high for 316N stainless steel.

Keywords: *316F, 316L, 316N crack depth, crack length, bursting pressure, ASME B31G, heat treatment.*

----------***----------

1. INTRODUCTION

Pipelines are widely used for water, crude oil, and natural gas transportation. The efficiency of the pipelines is attributable to their integrity and safety. Pipeline corrosion occurs naturally, due to the gradual and continuous environmental attack on pipe materials. It can happen on inside as well as outside surfaces. Pipe materials affected by corrosion include metal and non-metal pipes, pipe joints, welds and surface coatings. An example of pipeline corrosion is metal rusting in the presence of moisture and oxygen, which results in the formation of oxide of the metal (figure 1). Although literature on fracture mechanics of pipe lines is abundant, there is no estimation method that is accurate and broadly accepted. Using the von Mises yield criterion and the plastic instability theory, Cooper [1] and Svensson [2] presented a theoretical solution for the prediction of the burst pressure of cylindrical and spherical vessels. ASME B31.4 provides procedures for calculating the acceptability of various flaw types for steel gas pipelines [3]. The 316 stainless steel is an austenitic chromium-nickel stainless steel containing molybdenum. This addition increases general corrosion resistance, improves resistance to pitting from chloride ion solutions, and provides increased strength at elevated temperatures.

Figure 1: Corrosion crack.

The present work was motivated to optimize safety criteria for pressurized thin 316 stainless steel tubes. The present study was concerned about the severity of crack dimensions in crack propagation.

2. MATERIAL AND METHODS

The material of pipes was 316 stainless steel. The chosen control parameters are summarized in table 1. The control factors were assigned to the various columns of orthogonal array (OA), L9 is given in table 2. There have been many arguments on the corrosion shapes assumed by the design standards. Corroded area has been argued from as simple shape as a rectangle to parabolic (figure 2).

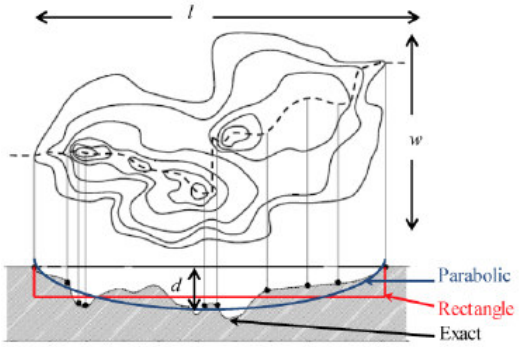

Figure 2: The crack dimensions.

Table 1: Control factors and their levels

Factor	Symbol	Level–1	Level–2	Level–3
Thickness, mm	A	1.0	1.2	1.5
Length of crack, mm	B	25	50	75
Depth of crack	C	30%t	40%t	50%t
Type of stainless steel	D	316F	316L	316N

where t is pipe thickness

Table 2: Orthogonal Array (L9) and control factors

Treat No.	A	B	C	D
1	1	1	1	1
2	1	2	2	2
3	1	3	3	3
4	2	1	2	3
5	2	2	3	1
6	2	3	1	2
7	3	1	3	2
8	3	2	1	3
9	3	3	2	1

The ASME B31G covers flaws in pipelines where flaws are the result of in-service corrosion processes [3]. The method is based on the "Dugdale Plastic Zone Model", the Folias factor M_f and an empiricism-based definition of defect depth d. The data base used for parameter fittings consisted basically of thin-walled pipes with medium strength and high toughness. For elliptical shape defect having its length L, the bursting pressure can be estimated as follows:

$$P_b = \frac{2t}{D}\sigma_{flow}\left[\frac{1-\frac{2d}{3t}}{1-\frac{2d}{3tM_f}}\right] \quad (1)$$

for $0.893\frac{L}{\sqrt{Dt}} \le 4$

$$P_b = \frac{2t}{D}\sigma_{flow}\left[1-\frac{d}{t}\right] \quad (2)$$

for $0.893\frac{L}{\sqrt{Dt}} > 4$

$$\sigma_{flow} = 1.1SMYS \text{ and } M_f = \sqrt{1+0.8\left[\frac{L}{D}\right]^2\frac{D}{t}}$$

where, D and t are, respectively, the nominal outside diameter and thickness of the pipe.

When a thin walled cylinder is subjected to internal pressure, three mutually perpendicular principal stresses are developed in the cylinder materials, namely: hoop stress, radial stress, and longitudinal stress.

The hoop stress resists the bursting effect of the applied pressure, p. Total force on one half of the cylinder due to applied pressure is given by

$$F_{ph} = p \times \text{Projected Area}$$

$$F_{ph} = p \times d \times L \quad (3)$$

where, p is the internal pressure; d is the internal diameter; L is the length of cylinder; t is the thickness of the cylinder.

The resisting force in the cylinder walls is given by

$$F_h = 2 \times \sigma_h \times L \times t \quad (4)$$

where σ_h is the hoop stress.

Figure 3: Equilibrium forces for hoop stress

For the equilibrium of forces as shown in figure 3, equating (3) & (4) we get

$$2 \times \sigma_h \times L \times t = p \times d \times L$$

Hoop stress, $\sigma_h = \frac{p \times d}{2t}$ (5)

When the cylinder has closed ends the internal pressure acts on the ends to develop a stress along the axis cylinder, known as longitudinal stress.

Total force on the end of the cylinder due to internal pressure

$$F_{el} = p \times \text{Area} = \text{pressure x area}$$

$$F_{el} = p \times \frac{\pi d^2}{4} \quad (6)$$

The resisting force in the cylinder ends is given by

$$F_r = \sigma_l \times \pi \times d \times t \quad (7)$$

where σl is the longitudinal stress.

Figure 4: Equilibrium forces for longitudinal stress

For the equilibrium of forces as shown in figure 4, equating (6) & (7) we get

$$\sigma_l \times \pi \times d \times t = p \times \frac{\pi d^2}{4}$$

Longitudinal stress, $\sigma_l = \frac{p \times d}{4t}$ (8)

Since the longitudinal stress is smaller than the hoop stress, for computing bursting pressure the hoop stress is only considered.

Total bursting pressure, p = Intensity of radial pressure x projected area

$$= p \times d \times L \quad (9)$$

Resisting force offered by the section xx = $\sigma_h \times 2t \times L$ (10)

Equating (7) & (8) we get

$$p \times d \times L = \sigma_h \times 2t \times L$$

Theoretical bursting pressure, $p = \frac{\sigma_h \times 2t}{d}$ (11)

Theoretical bursting pressure is calculated by replacing the hoop stress with ultimate strength of the thin shell as follows:

$$p = \frac{\sigma_{us} \times 2t}{d} \quad (12)$$

Table 3: ANOVA summary of the bursting pressure

Source	Sum 1	Sum 2	Sum 3	SS	v	V	F	P
A	37.50	46.04	57.69	68.41	1	68.41	23514.65	41.00
B	45.73	49.09	46.41	2.1	1	2.1	721.84	1.26
C	57.32	46.60	37.31	66.83	1	66.83	22971.56	40.05
D	41.21	696.62	141.23	29.51	1	29.51	10143.51	17.68
e				0.0117	4	0.00291	1.00	0.01
T	181.77	838.36	282.64	166.862	8			100

Note: SS is the sum of square, v is the degrees of freedom, V is the variance, F is the Fisher's ratio, P is the percentage of contribution and T is the sum squares due to total variation.

3. RESULTS AND DISCUSSION

Table 3 gives the ANOVA (analysis of variation) summary of bursting pressure. Even if all the process parameters could satisfy the Fisher's test at 90% confidence level, only pipe thickness, crack depth and type of material had major role in the total variation of bursting pressure. The pipe thickness (A), crack depth (C) and type of stainless steel (D) offered, respectively, 41.00%, 40.05% and 17.68% in the total variation of the bursting pressure. The crack length (B) was insignificant.

Figure 5 shows the dependence of bursting pressure on the pie thickness. As the pipe thickness increased the pressure required to burst the pipe would increase. The bursting pressure decreased with the increase of crack depth (figure 6). The

required bursting pressure was high for 316N stainless steel as compared to 316F and 316L stainless steels (figure 7).

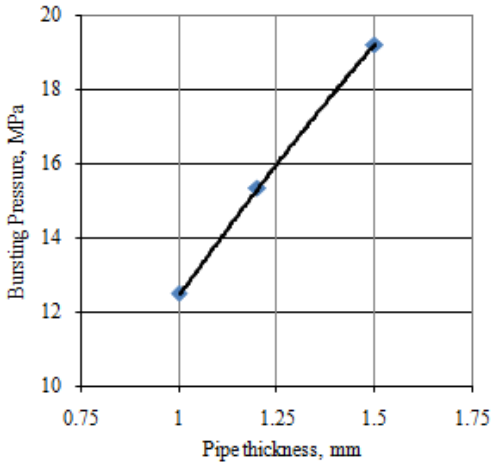

Figure 5: Effect of pipe thickness on bursting pressure.

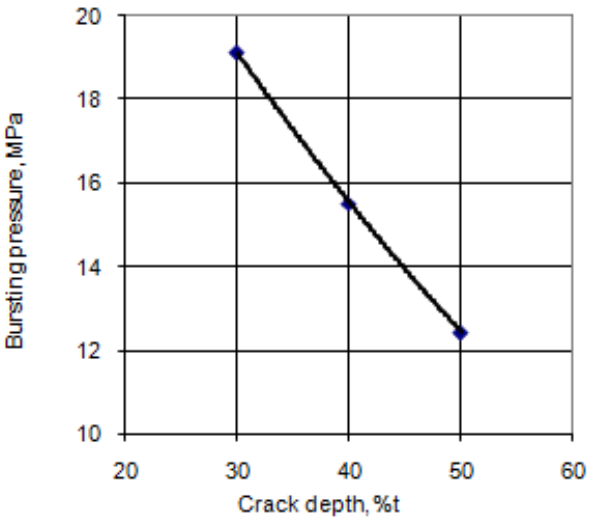

Figure 6: Effect of crack depth on bursting pressure.

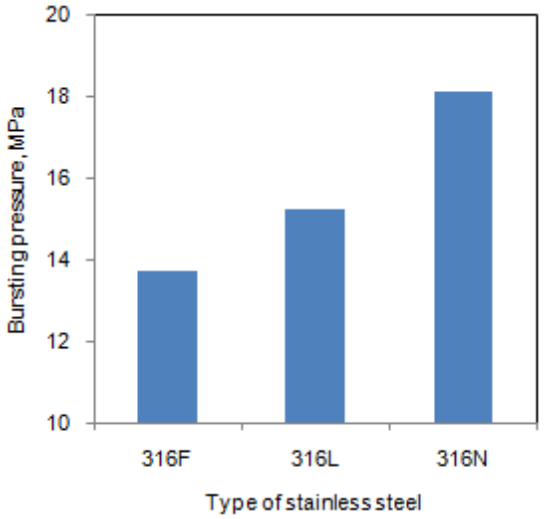

Figure 7: Effect of material on bursting pressure.

Table 4 gives the ANOVA summary of longitudinal stress. Even if all the process parameters could satisfy the Fisher's test at 90% confidence level, only crack depth and type of stainless steel had major role in the total variation of longitudinal stress. The crack depth (C) and type of material (D) offered, respectively, 77.13%, 40.05% and 22.54% in the total variation of the longitudinal stress. The pipe thickness and crack length (B) were insignificant.

Table 4: ANOVA summary of the longitudinal stress

Source	Sum 1	Sum 2	Sum 3	SS	v	V	F	P
A	232.15	232.14	229.78	1.24	1	1.24	1371.09	0.06
B	232.29	233.58	228.20	5.26	1	5.26	5816.09	0.27
C	279.45	230.35	184.27	1510.25	1	1510.25	1669914	77.13
D	207.58	17300.84	694.07	441.42	1	441.42	488086.9	22.54
e				0.003618	4	0.000904	1.00	0
T	951.47	17996.91	1336.32	1958.174	8			100

Table 5 gives the ANOVA summary of hoop stress. Even if all the process parameters could satisfy the Fisher's test at 90% confidence level, only crack depth and type of stainless steel had major role in the total variation of hoop stress. Incidentally, the crack depth (C) and type of material (D) contributed the same values of the total variation in the hoop stress. The pipe thickness and crack length (B) were insignificant.

Table 5: ANOVA summary of the hoop stress

Source	Sum 1	Sum 2	Sum 3	SS	v	V	F	P
A	464.30	464.28	459.56	4.98	1	4.98	1282.70	0.06
B	464.59	467.15	456.40	21.05	1	21.05	5421.84	0.27
C	558.90	460.70	368.54	6041.01	1	6041.01	155598	77.13
D	415.15	69203.37	1388.14	1765.68	1	1765.68	454785.3	22.54
e				0.01553	4	0.00388	1.00	0
T	1902.9	70595.50	2672.64	7832.704	8			100

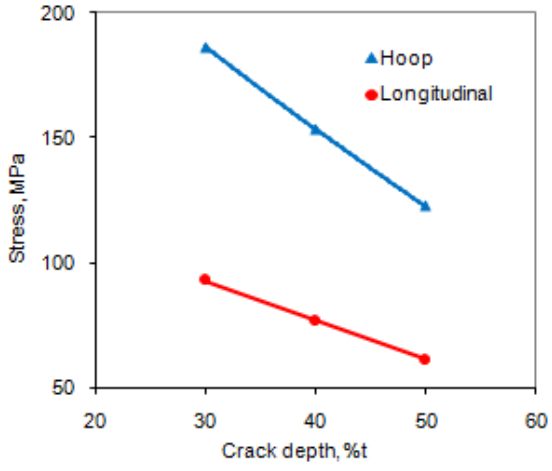

Figure 8: Effect of crack depth on longitudinal and hoop stresses.

The effect of crack depth on the longitudinal and hoop stresses is shown in figure 8. Both the longitudinal and hoop

stresses decreased with the increase of crack depth. The 316N stainless steel had higher longitudinal and hoop stresses than those of 316F and 316L (figure 9).

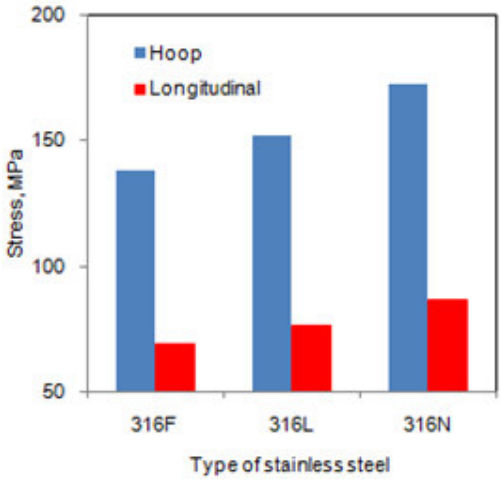

Figure 9: Effect of material on longitudinal and hoop stresses.

5. CONCLUSIONS

The bursting pressure is highly dependent on the pipe thickness and crack depth for 316 stainless steels. The bursting pressure increases with the increase of pipe thickness. Also, the bursting pressure decreases with the increase of crack depth. The longitudinal and hoop stresses are higher for 316N stainless steel than those of 316F and 316L stainless steels.

REFERENCES

[1]. W.E. Coope, The significance of the tensile test to pressure vessel design. Weld Journal, January 1957, pp.49–56.

[2]. N.L. Svensson, The bursting pressure of cylindrical and spherical pressure vessels, Transactions of ASME Journal of Applied Mechanics, vol.80, no.3, pp. 89–96, 1958.

[3]. American National Standards Institute (ANSI) / American Society of Mechanical Engineers (ASME): Manual for determining the remaining strength of corroded pipelines, ASME B31G, 1991.